Formation of metastable two-dimensional structures during Ag growth on Ge(100)

L. H. Chan and E. I. Altman
Department of Chemical Engineering, Yale University, New Haven, Connecticut 06520
(Received 28 February 2002; revised manuscript received 6 June 2002; published 31 October 2002)

Silver growth on Ge(100) between 330 and 570 K was studied using scanning tunneling microscopy. At 330 K, three-dimensional (3D) clusters along with two types of two-dimensional (2D) islands were observed: one elongated perpendicular to the substrate dimer rows, the other parallel to the dimer rows. The spacing and registry with the substrate of the former could be explained by Ag adatoms attaching across the substrate dimer bond, while the latter could be attributed to Ag ad-dimers. Annealing caused the larger 3D clusters to grow at the expense of the smaller 3D clusters and 2D islands; at 470 K the 2D islands were completely eliminated. Low-energy electron diffraction indicated that the 3D clusters were oriented with their (110) planes parallel to the surface. After annealing, the 3D clusters became elongated parallel to the Ge dimer rows indicating that the Ag[$\bar{1}$10] direction aligns parallel to the Ge $1\times$ direction. Although this suggested that the 3D clusters were lower in energy, Ag growth at 470 K led to two types of 2D islands along with pitting of the Ge surface; the pitting was taken as an indication that the islands were intermixed. Images of the islands revealed 2×3 and 3×2 periodicities. Images of the 3×2 structure showed a single maximum per unit cell, while images of domain boundaries showed that the 3×2 structure changed the outermost Ge layer. A model based on Ag-Ge mixed ad-dimers and Ag substitution into the Ge surface can explain these features. The 2×3 and 3×2 structures could only be seen after Ag deposition at ~470 K; both annealing films deposited at lower temperatures and higher growth temperatures created only 3D clusters. Thus formation of these intermixed structures was attributed to growth of metastable Ag-Ge nuclei at 470 K that were kinetically inhibited from forming at lower temperatures and whose lifetimes were too short to grow at higher temperatures.

DOI: 10.1103/PhysRevB.66.155339 PACS number(s): 68.55.Ac, 68.37.Ef, 68.35.Ct

I. INTRODUCTION

The Ag on Ge system is interesting because of the way the growth mode changes with temperature and because of its superconducting properties.[1–5] Early studies of Ag growth on Ge(100) near room temperature suggested that the growth mode is of Stranski-Krastanov (SK) type.[3] More recent scanning tunneling microscopy (STM) studies, however, showed that the growth mode is of Volmer Weber (VW) type at 300 K and of SK type at 100 K.[1,2] At 100 K the Ag islands were one atom high up to at least 1 ML, but as the substrate temperature was increased toward 300 K, three-dimensional (3D) clusters started to form on the surface. At both 100 and 300 K, Ag grew with its (110) face parallel to the Ge(100) surface in two domains.[3–5] The authors of Ref. 4 suggested that Ag adsorption lifted the Ge(100) surface reconstruction.[4] All studies of Ag growth on Ge(100) agreed that the interaction between Ag and the Ge substrate is weak with no evidence for surface intermixing. The weak interaction is also supported by the Ag-Ge bulk phase diagram that indicates that Ag is immiscible in Ge up to 924 K, and that the miscibility of Ge into Ag is low, less than 10-wt % Ge.[6] Thus it appears that the SK growth observed at low temperatures is due to kinetic limitations and that VW growth is the favored growth mode.

In this paper it will be shown that Ag nucleation on Ge(100) displays a very unusual temperature dependence. When Ag was deposited onto Ge(100) at 300 K, both 3D clusters and 2D islands were observed; annealing caused the 3D clusters to grow and the 2D islands to disappear, suggesting that the 3D clusters were lower in energy. When Ag was deposited at 470 K, however, two ordered 2D structures were observed along with voids in the Ge surface. The voids suggested that the 2D structures were Ag-Ge surface alloys. Surface intermixing has not been reported previously for Ag on Ge(100) to our knowledge; however, it has been seen in other systems that are immiscible in the bulk, including Ag and Au on Si(100).[7–9] The unusual aspect of Ag growth on Ge(100) is that the surface alloys were only observed after depositing Ag at 470 K. Both Ag deposition at lower temperatures followed by annealing to 470 K and holding the surface at 470 K after depositing Ag at that temperature led to only 3D Ag clusters.

II. EXPERIMENT

Experimental procedures and equipment were described previously.[10–12] Briefly, experiments were performed using an ultrahigh-vacuum system equipped with an energy analyzer for Auger electron spectroscopy (AES), an ion gun for sputtering, low-energy electron-diffraction (LEED) optics, resistively heated evaporation sources, a quartz crystal deposition rate controller, and a scanning tunneling microscope.[13]

The Ge samples were nominally undoped with a resistivity of 50–60 Ω cm. Atomically flat surfaces with large evenly spaced terraces were obtained by sputter/anneal cycles until all contaminants were below the AES detection level, then depositing a Ge buffer layer at 630 K, and then a final anneal at 920 K.[12]

Silver was deposited at rates between 7 and 9 $\times10^{12}$ atoms/cm^2 sec. The Ag coverage was calculated according to the bulk Ag(110) plane so that 1-ML Ag contains 8.47×10^{14} atoms/cm^2 and is 0.144 nm thick.

All STM images were acquired at room temperature. Images were obtained at tunnel currents between 0.1 and 1.0

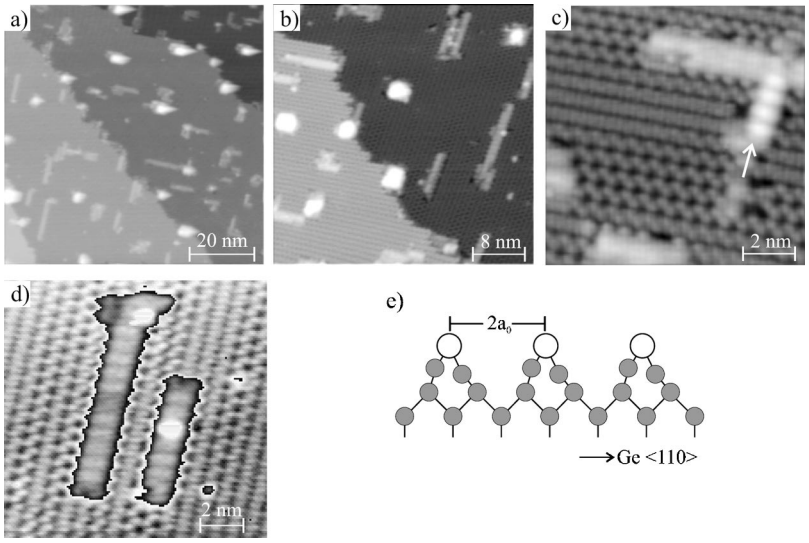

FIG. 1. STM images (a)–(d) of the Ge(100) surface after depositing 0.05 ML of Ag at 330 K. The images were obtained with $V_s = -1.5$ V. The contrast was enhanced in (d) by cycling through the gray scale twice. (e) Schematic showing a side view of the surface with Ag adatoms (large open circles) attaching across the Ge dimers. The schematic explains the bead-like structure pointed to in (c).

nA, and sample biases between -3 and $+3$ V. Throughout this paper, sample biases are reported so that negative biases refer to occupied states and positive biases unoccupied states. Varying the tunnel current was not found to affect the STM images significantly. Where noted, the contrast in the images was enhanced by cycling through the gray scale twice; this allows the three-dimensional clusters and the terrace structure to be seen in a single image.

III. RESULTS

A. Ag growth on Ge(100) at 330 K

After 0.05 ML of Ag was deposited onto Ge(100) at 330 K, the surface morphology was characterized by 2D islands and 3D clusters, as shown in Figs. 1(a) and 1(b). The appearance of the upper right corner of the 3D clusters in Fig. 1(a) is due to a tip artifact. The 3D clusters had an average apparent height of 0.55 nm, which corresponds to 4 ML of Ag(110) though electronic differences between the clusters and the substrate make this is a rough estimate. Most of the 2D islands were elongated parallel to the substrate dimer rows with an average apparent height of 0.12 nm. Figure 1(d) shows that these islands are made up of chains with a $2\times$ periodicity parallel to the chain and pairs of maxima perpendicular to the chains. There were exceptions, however, where beadlike structures formed perpendicular to the dimer rows as indicated by the arrow in Fig. 1(c), these features appeared 0.17 nm higher than the other 2D islands. While prior STM work on Ag growth near room temperature revealed 2D and 3D structures, the bead like structures were not observed.[2] The beads were 0.8 nm apart, the same distance that separates the Ge dimers in the $2\times$ direction, and were aligned off center over the substrate dimer rows. A structural model that explains these features is illustrated in Fig. 1(e). In this model, Ag atoms add across the Ge dimer bond with tilt towards one of the Ge atoms accounting for the asymmetric appearance. The model closely corresponds to one proposed in a recent theoretical study of Ag adsorption on Ge(100).[14]

Annealing caused both the 2D island and 3D cluster densities to decrease. When a surface with 0.05 ML of Ag deposited at 330 K was annealed to 470 K for 2 min, all of the 2D islands disappeared, as shown in Figs. 2(a) and 2(b). In Fig. 2(a), the Ge substrate showed no obvious changes, such

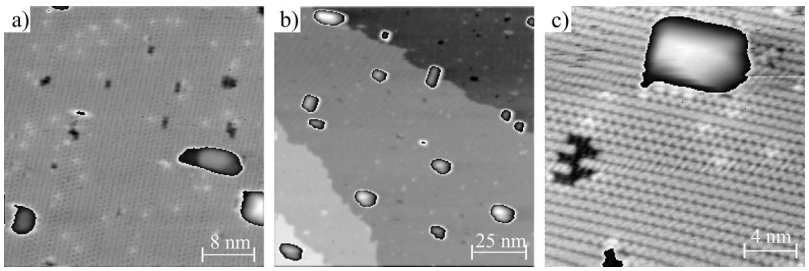

FIG. 2. STM images of a Ge(100) surface with 0.05-ML Ag deposited at 330 K obtained after annealing at 470 K for 2 mm. The contrast in the images was enhanced by cycling through the gray scale twice, so that substrate features could be seen more clearly. The images were obtained with $V_s = -1.5$ V.

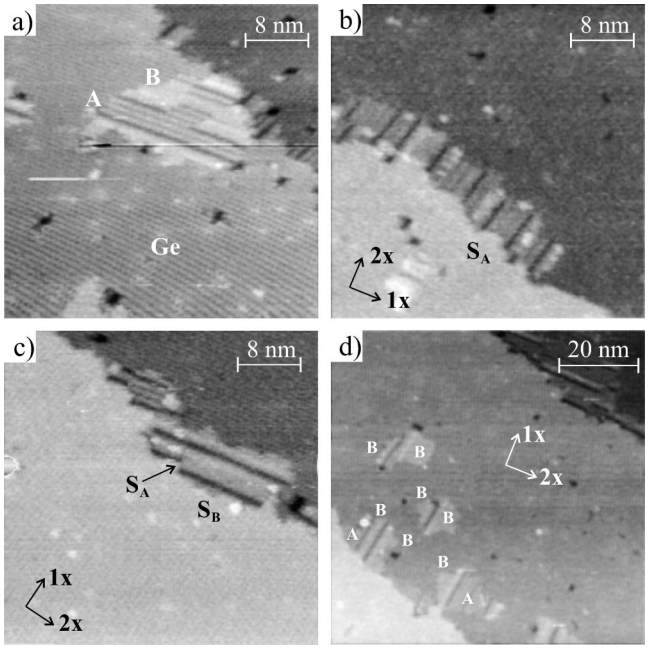

FIG. 3. STM images obtained after depositing 0.05-ML Ag at 470 K. (a) Image showing two distinct types of islands labeled *A* and *B*. (b) Image showing preferential attachment of islands to an S_A step. (c) At S_B steps the islands attach to kinks that form S_A step segments and leave a gap between the island edges and the step edges. (d) On the terraces the islands consist of multiple domains with domain boundaries seen between island edges that taper in opposite directions; the markers label the different types of islands. The images were obtained with $V_s = (a) -1.25$ V, (b) -1.5 V, (c) -1.5 V, and (d) -1.25 V.

as pit formation, so there was no evidence of surface intermixing. Figure 2(b) shows a larger area of the surface, 120×120 nm^2. This image shows that some of the 3D clusters appeared more rectangular. On average, after annealing the aspect ratio of the clusters increased from 1.29 ± 0.25 to 1.66 ± 0.46. These values were obtained from a number of images of the surface before and after annealing, the aspect ratios in Figs. 1(a) and 2(b) average 1.3 and 1.5, respectively. The clusters also grew vertically with the average apparent height increasing from 0.55 to 1.7 nm. The rectangular shape is consistent with the reports of Ag(110) growth on Ge(100),[4] and at higher coverages the LEED pattern expected for Ag(110) was observed. In this case, the longer sides of the cluster are expected to parallel the more densely packed Ag$[\bar{1}10]$ direction. Figure 2(c) shows that the longer edges of the clusters tend to parallel the substrate dimer rows indicating that Ag$[\bar{1}10]$ preferentially aligns parallel to the Ge(100) $1\times$ direction.

B. Initial Ag growth on Ge(100) at 470 K

Since only 3D clusters were seen after annealing to 470 K, the 3D structures were presumed to be lower in energy. Therefore, increasing the growth temperature was also expected to eliminate all 2D structures. This, however, was not the case. Instead, raising the temperature to 470 K led to two types of 2D structures. As shown in Fig. 3, after depositing 0.05 ML of Ag at 470 K, patches of 2D islands with two major types of features were observed. One type, identified as *A*, consisted of stripelike features that paralleled the substrate dimer rows as indicated in Fig. 3(a). The distance between the stripes was 1.2 nm, yielding a $3\times$ periodicity with respect to bulk-terminated Ge(100). A different type of island, identified as *B*, coexisted with the type-*A* islands but could not be resolved in atomic detail from these images. Type-*B* islands appeared slightly higher than the type-*A* islands, by 0.1 nm in Fig. 3(a), while the type-*A* structures appeared 0.05 nm above the Ge terraces. These numbers are provided to give an indication of the corrugation; because of electronic differences between the islands and the substrate, these heights do not represent true topographic variations.

Both *A*- and *B*-type islands preferentially attached to step edges, as shown in Figs. 3(b) and 3(c). On the Ge(100) 2×1 surface, steps are generally classified into two types: S_A steps where the dimer rows on the upper terrace parallel the step edge, and S_B steps where the dimer rows on the upper terrace are perpendicular to the step edge.[15] The islands grew immediately under S_A step edges [Fig. 3(b)] without any observable gap, while at S_B steps a minimum separation of 1.6 nm was seen between the islands and the step. A section of the islands could be seen to attach to a segment of the step without any gap in Fig. 3(c) as indicated by the arrow. This segment, however, is actually a short S_A step.

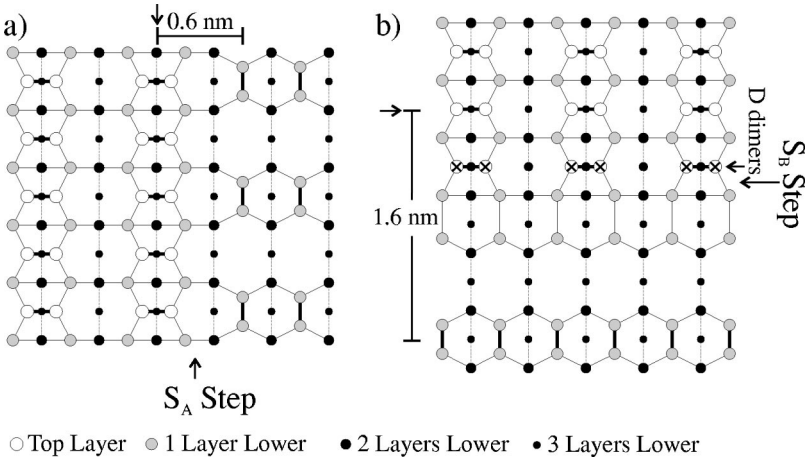

FIG. 4. Schematics showing the favored atomic arrangements at (a) S_A and (b) S_B steps. The *x*'s in (b) mark the last row of dimers on the upper terrace. These appear dim in occupied state STM images (Refs. 16 and 19).

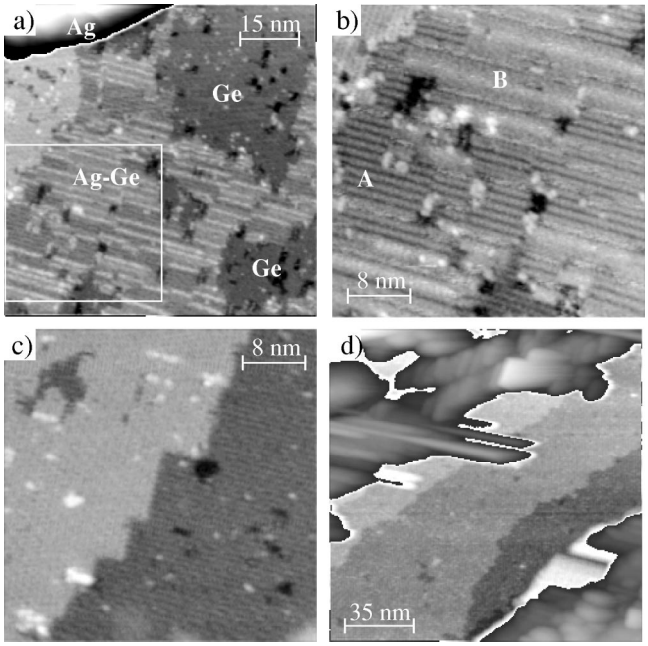

FIG. 5. Images of a Ge(100) surface with 0.34 ML of Ag deposited at 470 K before [(a) and (b)] and after [(c) and (d)] annealing at 470 K for 30 min. The box in (a) highlights the area shown in (b). The markers *A* and *B* denote two different types of Ag-induced islands, while Ge marks areas that expose the substrate, and Ag 3D Ag clusters. The images were obtained with $V_s = -1.5$ V (a), -1.25 V (b), -2.0 V (c), and -1.25 V (d). In (a) and (d) the gray scale was cycled through twice to allow the terraces and 2D islands as well as the 3D clusters to be seen simultaneously.

The different behavior at the two step edges can be understood by considering the available bonding sites adjacent to the steps as illustrated in Fig. 4. At the S_A step, the first pair of unperturbed dimers on the lower terrace is only 0.6 nm [Fig. 4(a)] from the last dimers on the upper terrace. In the favored termination of S_B steps shown in Fig. 4(b), the last dimers at the upper step edge are electronically different and as a result appear as dim shadows in occupied state STM images.[16–19] This gives the false impression that the steps terminate one dimer sooner than they actually do.[16] On the lower terrace, the rows of Ge atoms beneath the step bond with the next row of atoms to form a ''rebonded step edge.'' [15,16] Thus when crossing an S_B step the distance between the last visible dimer on the upper terrace and the first unperturbed dimer on the lower terrace in occupied state images, such as those in Fig. 3, is 1.6 nm. Therefore, the results indicate that the rebonding at S_B steps renders the Ge atoms at the bottom of the step unreactive towards Ag at 470 K, and that Ag preferentially attaches to the first unperturbed dimers on the lower terrace.

The wider range image in Fig. 3(d) shows several islands on the terraces. Although the island density is low, each of the islands has at least one domain boundary. Interestingly, the *B*-type islands taper in opposite directions when the domain boundary is crossed.

C. Continuing Ag growth on Ge(100) at 470 K

When the Ag coverage was increased to 0.34 ML at 470 K, more islands were observed and pits began to grow on the surface as shown in Fig. 5(a). There were also large elongated 3D clusters with heights ranging between 3 and 5 nm scarcely distributed across the surface. The feature at the upper left corner of Fig. 5(a) is part of one such cluster. The upper right corner of the image shows the bare Ge surface with many pits; toward the center of Fig. 5(a) were the islands. Zooming into the white square, Fig. 5(b) shows more details of these islands. The type-*A* islands appear lower and the type-*B* islands less well resolved. Although only 0.34 ML of Ag was deposited and some of the Ag went into the 3D clusters, the type-*A* and -*B* structures covered more than 50% of the Ge surface. This disproportionately high coverage compared to the amount of Ag deposited could be due to adsorbate structures in which the Ag atoms are much further apart than the 0.289 nm favored in bulk Ag, or to integrating Ge atoms into the structures to form Ag-Ge surface alloys. The pits and the lack of any Ge islands support the latter. It is unlikely that the Ge from the pits incorporated into the 3D clusters because annealing Ag-covered surfaces formed at lower temperatures produced similar (110)-oriented Ag clusters without pitting. Further, the area of the pits would suggest a Ge content in the Ag clusters that exceeds the bulk miscibility. These structures were different from the 2D islands seen at 330 K. At 330 K, there was no pitting and the 2D islands showed no preference for step edges.

When the surface was held at 470 K for a prolonged period after deposition at this temperature, both the *A*- and *B*-type structures disappeared, as shown in Fig. 5(c). The Ge(100) 2×1 reconstruction was restored, but a few large pits remained and the step edges were modified. The persistence of the pits could be accounted for by some of the Ge atoms liberated from the dissociated islands attaching to preexisting steps rather than filling the pits. The growth of the few remaining pits can be attributed to Ostwald ripening during annealing. The Ag aggregated into large, elongated 3D clusters, as shown in Fig. 5(d). The high aspect ratio of the clusters made them difficult to image; however, their existence and general shape were still obvious in the images.

As the Ag coverage increased to 0.73 ML at 470 K, the size and density of the 3D clusters increased, reducing the coverage of the flat areas by the 2D islands. The flat areas were still characterized by type-*A* and -*B* islands, bare Ge and pits. The biggest change in these features was that the pits became organized into narrow strips running perpendicular to the substrate dimer rows as shown in Figs. 6(a) and 6(b). These narrow trenches tended to locate adjacent to type-*A* islands and in the bare Ge sections of the surface. In addition, bright stripes on the top of type-*B* features could be observed, as indicated by the arrow in Fig. 6(b).

In prior work on Ag on Si(100), narrow trenches were also seen after depositing Ag. On Si, the trenches were seen prior to the islands and so it was suggested that they were caused by stress relief due to Ag incorporation into the 2×1 Si surface.[20] Here the trenches were only seen when the *A* and *B* islands formed on the surface, and the trench coverage increased as the islands grew. This suggests that the islands incorporate both Ag and Ge rather than just the Ge surface. The type-*A* features, in particular, were found adjacent to either step edges or the narrow trenches suggesting

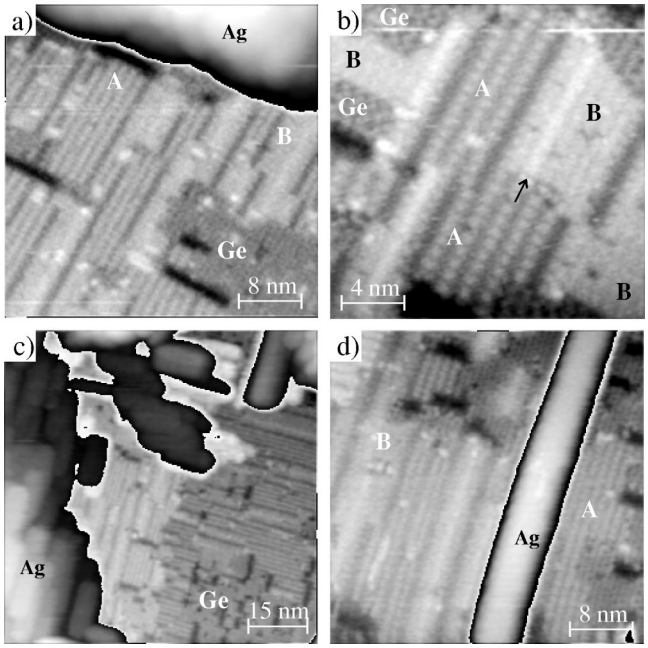

FIG. 6. STM images of the Ge(100) surface obtained after depositing 0.73 ML [(a) and (b)] and 1.4 ML [(c) and (d)] of Ag at 470 K. In (a), (c), and (d), the contrast was enhanced by cycling through the gray scale twice, so that features on the terraces could easily be resolved. The markers denote two types of islands, the bare Ge substrate, and 3D Ag clusters. The images were obtained with $V_s = -2.0$ V [(a) and (b)] and -1.25 V [(c) and (d)].

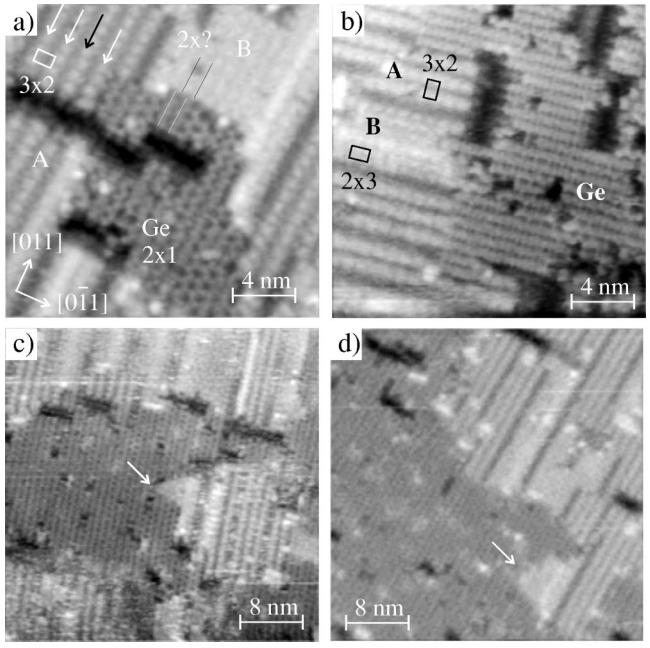

FIG. 7. (a) and (b) High-resolution STM images of the type-*A* and -*B* structures reveal 3×2 and 2×3 periodicities, respectively. The boxes highlight the unit cells and the arrows in (a) highlight where one row of the 3×2 structure is out of registry with the other rows. (c) and (d) Wider range images show that the more isolated 2×3 type-*B* islands tend to be diamond shaped, as highlighted by the arrows. The surface was prepared by depositing 0.73-ML Ag at 470 K. The images were obtained with $V_s = -2.0$ V.

that the type-*A* islands pulled Ge atoms from the surface and were most likely Ge rich. Unfortunately, the heterogeneity of the surface limited the utility of surface analytical techniques to determining the composition of the individual phases.

At a higher Ag coverage of 1.4 ML, the surface structure and morphology did not significantly change. The 3D clusters grew larger and longer, as shown in Figs. 6(c) and 6(d) while the coverage of the 2D structures declined. Figure 6(d) shows a typical elongated 3D cluster that had an apparent height of 1.2 nm and was at least 40 nm long, running parallel to the substrate Ge dimer rows. Despite the high Ag coverage, a significant fraction of the Ge surface remained bare as shown near the lower right corner of Fig. 6(c).

The 3D clusters were the final structure at both high coverage and after prolonged annealing at the 470-K growth temperature. Deposition at 570 K was also studied. At a low Ag coverage of 0.04 ML, no islands were seen at the step edge and the density of 3D Ag clusters was very low and so images of this surface were indistinguishable from those of the clean surface. At a higher coverage of 0.7 ML at 570 K, the images were similar to Fig. 5(d) with large 3D clusters that were difficult to image and no evidence of the type-*A* and -*B* structures on the flatter areas. Therefore, the formation of type-*A* and -*B* structures was restricted to Ag deposition in a narrow substrate temperature window around 470 K.

D. High-resolution and bias-dependent imaging of Ag islands grown at 470 K

The structural details of the type-*A* and -*B* islands can be seen more clearly in the small range STM images shown in Fig. 7. The type-*A* structure had a 3×2 periodicity, as shown in the upper left corner of Fig. 7(a). The convention here in denoting the periodicity is that the first number always parallels the Ge(100)$2\times$direction. Low-energy electron-diffraction patterns after deposition at 470 K showed an increased diffuse background, spots that could be associated with diffraction from (110)-oriented Ag clusters, and streaking along the (1,0) and (0,1) directions but no distinct spots that could be associated with a 3×2 periodicity. The lack of distinct 3×2 spots was due to the small size of the domains as well as disorder due to the poor registry between the rows. The arrows in the upper left corner were drawn to illustrate where three (white arrows) out of four rows of the 3×2 structure are in registry while the fourth was shifted one surface lattice constant along the island $2\times$ direction as indicated by the black arrow. In addition, the $3\times$ direction was often skipped, also weakening diffraction from the 3×2 islands.

The type-*B* structure was more difficult to resolve with STM and its appearance varied significantly depending on the tip condition and bias. In the upper center of Fig. 7(a) a $2\times$ periodicity shifted one surface lattice constant with respect to the substrate Ge dimer rows can be observed in the substrate $2\times$ direction. In some STM images, such as Fig. 7(b) the periodicity in the substrate $1\times$ direction could be resolved as a $3\times$ periodicity. This gave the type-*B* structure a 2×3 unit cell. The type-*B* islands also tended to be small with many imperfections that would again account for the lack of any 2×3 or 3×2 LEED pattern. When the type-*B*

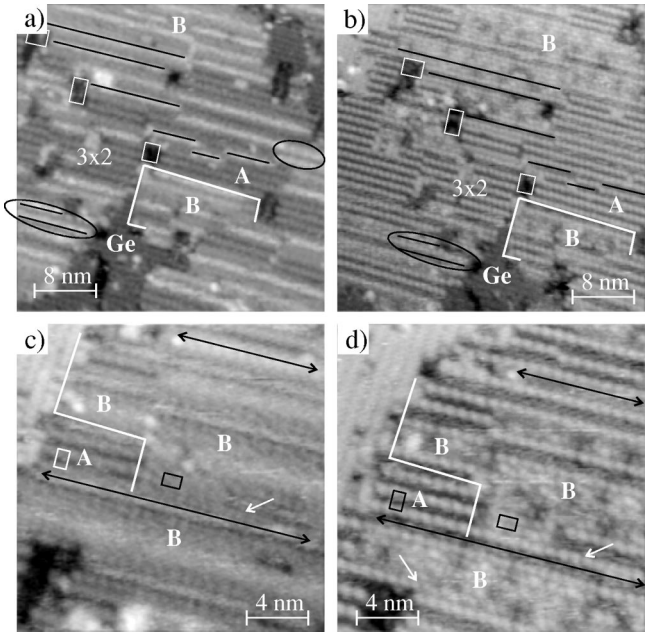

FIG. 8. Comparison of empty [(a) and (c)] and filled-state [(b) and (d)] STM images of the same area of a surface with Ag-induced islands formed at 470 K. The lines and boxes highlight where the same features appear in (a) and (b) and (c) and (d). The images were obtained with (a) $V_s = 1.0$ V, empty states; (b) -1.5 V, filled states; (c) 1.0 V, empty states; and (d) -1.25 V. The Ag coverage was 0.34 ML.

islands were more isolated, they tended to exhibit angular shapes with edges preferentially aligned along substrate $\langle 310 \rangle$ directions as highlighted by the arrows in Fig. 7(c) and 7(d).

The effect of the imaging bias on the appearance of the 3×2 and 2×3 structures is illustrated in Fig. 8 which shows a comparison of occupied and unoccupied state images of the same area. Both the corrugation within the 3×2 and 2×3 structures and their heights above the bare Ge surface are much less in the unoccupied state images [Figs. 8(a) and 8(c)] than in the occupied state images [Figs. 8(b) and 8(d)]. Also, the unoccupied state images show a number of ridges that can be clearly seen as bright lines in Fig. 8(a). The width and height of these lines depended on the bias voltage. When filled states were imaged in the same areas, Fig. 8(b) shows that the white lines appeared as depressions. In Fig. 8(b), it becomes apparent that these ridges appear at boundaries between 3×2 domains where the spacing between the rows is expanded to $4\times$ and at boundaries between *A* and *B*-type structures. Figures 8(c) and 8(d) show another pair of empty/filled state images of the same area at higher resolution. It can be seen more clearly that some of the 3×2 strings extend along the edges and through the *B*-type domains as indicated by the arrows. The 2×3 periodicity in the *B*-type structure could be observed in a small area in Fig. 8(d). Here it can be seen that the order of the 2×3 structure does not extend beyond four unit cells, which helps explain the absence of any 2×3 LEED pattern.

IV. DISCUSSION

A. Temperature dependence of Ag growth on Ge(100)

Silver growth on Ge(100) goes through the following sequence as the temperature is increased: (1) 2D island growth at 120 K (Ref. 1), (2) 3D cluster growth in competition with 2D island growth at 330 K, (3) 3D cluster growth in competition with 2D Ag-Ge alloy formation at 470 K, and (4) 3D cluster growth above 470 K. The transition from 2D to 3D island growth as the temperature is raised toward 300 K can be understood in terms of kinetic limitations. In considering nucleation, a critical size is defined above which clusters can decrease their free energy by growing. The free energy, however, also depends on the cluster geometry and so there is actually a series of curves that define the free energy dependence on size for different geometries. If the temperature is high enough for the clusters to rapidly restructure so that they always adopt the minimum energy configuration, then the series of curves collapse to a single curve. Initial growth on surfaces occurs via adatoms colliding with the periphery of the clusters and so formation of 3D nuclei requires interlayer transport that can be kinetically inhibited at low temperatures. As a result, at low temperatures 2D islands can grow and become stable. As the temperature is increased, the rate of 2D island restructuring to lower-energy 3D configurations becomes comparable to the growth rate and thus a regime is reached where 2D growth competes with 3D cluster formation. For Ag on Ge(100), this occurs near 300 K.

The above model suggests that continuing to increase the temperature should lead to only 3D clusters. This, however, was not the case. At 470 K, 2D islands emerged. Their simultaneous appearance with pits in the Ge surface indicated that these 2D phases contained both Ag and Ge. This suggests that increasing the temperature to 470 K opened up a kinetic pathway that included extracting Ge atoms from the surface layer. In other systems where surface intermixing occurs, a similar threshold temperature was observed below which only growth on top of the surface is seen.[21–24] Therefore, this result is not unusual.

What is unusual is that the 2D Ag-Ge phases were only seen following deposition at 470 K. Increasing the growth temperature, annealing films deposited at lower temperatures, and holding the surface at 470 K after stopping growth at the same temperature all produced only 3D clusters. These observations point toward the 3D clusters being the lowest energy configuration. The formation of the higher-energy Ag-Ge phases can be understood along the same lines as the growth of the 2D Ag islands at low temperatures. As the temperature is increased toward 470 K, a kinetic pathway is opened that allows intermixed islands to be created. The energy of the island edges causes the free energy of formation of the 2D Ag-Ge islands to go through a maximum as their size is increased and thus there will be a critical size above which the islands will be stable. Although the 3D Ag clusters are lower in energy, a barrier to restructuring and eliminating Ge can allow the 2D Ag-Ge islands to grow. Thus increasing the temperature to $\sim$470 K allows Ag-Ge islands to form, but at higher temperatures their lifetimes can be too short for them to grow.

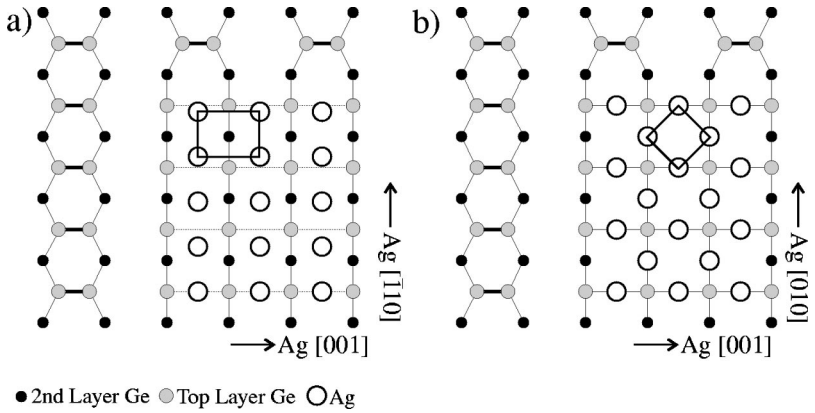

FIG. 9. Models illustrating the epitaxial relationship between (a) Ag(110) and (b) Ag(100) with Ge(100). In both cases, the Ag is presumed to lift the reconstruction. The 2×1 reconstruction is shown adjacent to the Ag islands to indicate the Ge bonding directions.

The changes that occur on annealing can be associated with Ostwald ripening. In this case, the island and cluster free energies depend on their geometry as well as their size, and so the 3D clusters grow at the expense of the 2D islands. Interestingly, these observations suggest that at 470 K Ag atoms are emitted from the 2D islands and 3D clusters and diffuse across the surface. Therefore, we might have expected to see 2D Ag-Ge islands after annealing films deposited at lower temperatures. The densities of the surface species, however, are very different during the initial stages of growth and ripening. When growth is started the adatom density will be much higher while there are far fewer existing clusters that the adatoms can attach to. Thus during annealing the probability of Ag adatom collisions may simply be too low to nucleate Ag-Ge islands.

B. Structure of clusters and islands formed during Ag growth on Ge(100)

The 3D clusters have previously been observed with STM (Ref. 2) and the (110) orientation was presumed based on reflection high-energy electron-diffraction (RHEED) studies.[4] In prior work, it was shown that the Ag clusters were elongated in the Ag[$\bar{1}$10] direction.[2] From our STM images, it became obvious that the clusters preferentially align so that their [$\bar{1}$10] direction parallels the Ge(100) $1\times$ direction and their [001] direction the Ge(100) $2\times$ direction. This can be understood as the spacing along Ag[001] is 0.409 nm which closely matches the 0.400 nm atomic spacing on a 1×1 Ge(100) plane. Since the bonds from the surface Ge atoms extend out of the surface along the $2\times$ direction of the reconstruction, this alignment places rows of Ag atoms above the dangling bonds of the Ge atoms, as illustrated in Fig. 9(a). The Ag clusters are pictured as sitting on top of a 1×1 surface in Fig. 9; however, the structure of the underlying surface could not be determined from the STM images. In the RHEED study it was presumed that Ag lifted the reconstruction.[4] Because the spacing along the Ag[$\bar{1}$10] direction (0.289 nm) is much less than the Ge(100) spacing, the registry between the Ag clusters and the substrate is poor along the non-bonding $1\times$ direction. Therefore, it might appear that Ag would ''prefer'' to grow with its [001] and [010] directions parallel to Ge[011] and [0$\bar{1}$1]. As shown in Fig. 9(b), however, this would place one Ag atom per unit cell either directly above a Ge atom or between Ge atoms where there are no dangling bonds. This apparently is more unfavorable than the mismatch and so (110)-oriented clusters from instead.

Recently, Seino and Ishii used density-functional calculations to evaluate different bonding geometries of Ag adatoms and ad-dimers on Ge(100) and to calculate STM images based on the density of states.[14] For adatoms, they found three structures that were too close in energy to be distinguished, including one in which Ag atoms bond across the Ge dimer bond, as shown in Fig. 1(e). This model explains the periodicity and registry with the substrate of the beadlike islands seen after growth at 330 K. Further, the STM images of these islands are very similar to the theoretical predictions. Seino and Ishii also suggested that higher Ag densities favor a dimerization of the Ag atoms, with Ag dimers parallel to the substrate Ge dimers lower in energy. This suggests that the beadlike islands were due to individual adsorbed Ag atoms while the islands that were elongated parallel to the Ge dimer rows were due to Ag dimers. In prior work, unoccupied state images of the latter revealed oval features on the islands.[2] In filled-state images we resolved pairs of maxima on the chains and a $2\times$ periodicity perpendicular to the chains, consistent with parallel dimers occupying every other site along the substrate $1\times$ direction as suggested by Kushida *et al.*[2] Interestingly, the energy of a Ag atom replacing one of the atoms in a Ge dimer was also calculated and it was concluded that such a configuration is metastable because it is only 0.17 eV above the adatom configurations.

Although the 3×2 and 2×3 surface structures were readily identified by STM, determining the atomic structure and composition of these phases is difficult. Because these phases always coexisted with 3D Ag clusters, the bare Ge surface, and one another, they could not be unambiguously characterized using surface analysis techniques. Still, the simultaneous growth of pits and the 3×2 and 2×3 islands indicated that these were alloy phases. In this regard, Ag growth on Ge and Si(100) share some similarities. On Si(100), a 2×3 structure was observed along with pitting after either depositing Ag between 770- and 870 K[25,26] or annealing a Ag layer deposited at room temperature to 620–770 K.[7,27] At lower Ag coverages, diamond-shaped 2×3 islands with edges oriented along substrate (310) directions

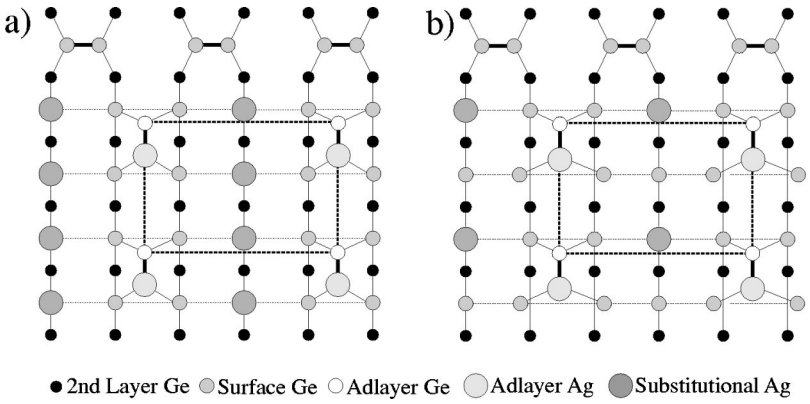

FIG. 10. Proposed substitution plus Ag-Ge ad-dimer models for the 3×2 Ag-induced islands formed at 470 K. The dashed boxes highlight the 3×2 unit cells. The models show the islands adjacent to the 2×1 substrate terraces to indicate the registry of the structure with the substrate. In (a), Ag completely replaces the Ge atoms in the substrate row between the ad-dimers, while in (b) every other Ge atom is replaced by Ag leaving one Ge atom per unit cell nominally with two dangling bonds. To compensate for this, the model shows the neighboring Ge atoms relaxing toward this Ge atom.

were observed.[7] The 2×3 islands on Ge(100) favored the same shape and on both surfaces domain boundaries were observed between segments of islands tapered in opposite directions. There are, however, also some differences between the (2×3)-Ag on Si and Ge(100). On Si, the 2×3 structure appears more corrugated in empty-state images and the maxima display a triangular shape.[7] The triangular shape eliminates a mirror plane in the $3\times$ direction accounting for the observed domain boundaries. Similar features in the islands on Ge(100) also suggest the lack of a mirror plane though no asymmetry in the maxima could be resolved. Although the data indicate that the 2×3 structures are not identical on Si and Ge(100), the similarities suggest that the structure on the Si surface can be used as a starting point for understanding the structure on Ge.

Whether the 2×3 structure on Si(100) is a Ag adlayer or a Si-Ag alloy layer has been debated.[7,25,26,28] The study by Michely *et al.*, however, provided convincing evidence that the (2×3) phase is an alloy.[26] In their work they prepared a Si(100) surface containing many Si islands and showed using low-energy electron microscopy (LEEM) that these islands were consumed to produce the 2×3 phase and recreated when Ag desorbed. Further, their medium energy ion scattering (MEIS) data for a surface completely covered by the 2×3 phase put the composition of this phase at 50% Ag. Although several models have been proposed, the structure of the 2×3 phase on Si remains uncertain. A couple of the models are based on Ag overlayers with coverages of $\frac{1}{3}$ and $\frac{2}{3}$ ML that are not consistent with the LEEM and MEIS data.[25,28] On the other hand, a model based on $\frac{1}{2}$-ML Ag with three Ag and three Si atoms per unit cell[26] is contradicted by angle-resolved photoelectron spectroscopy (ARPES) and x-ray photoelectron diffraction (XPD) results.[27,28] The XPD data showed poor agreement with the model while ARPES showed a large band gap that was inconsistent with a unit cell with an odd number of electrons. Our bias study revealed the diminution of the 2×3 and 3×2 islands on Ge(100), also suggesting the existence of a bandgap that can put a constraint on the composition of the islands.

Unlike the 2×3 structure, there is no obvious analog of the 3×2 structure on Si(100). The STM images provide insight into the 3×2 structure in addition to the periodicity. Because the registry between the rows is poor, the structure cannot depend strongly on the alignment of the 3×2 rows. Also, the images of the domain boundaries suggest that the structure involves a change in the outermost Ge layer. In particular, at the bottom left of Fig. 7(b) there are two domain boundaries where there is enough space for the Ge dimer rows to continue through the islands but instead the rows terminate near the island edge. The raised appearance of the domain boundaries in unoccupied state images reinforces this conclusion. Based on these observations and the calculations that classify mixed Ag-Ge dimers as metastable,[14] we propose a model based on Ag substituting into the outermost Ge layer and Ag-Ge ad-dimers. Two such models are pictured in Fig. 10. In Fig. 10(a) there are three Ag atoms per unit cell, and so such a structure would be expected to be metallic, while in Fig. 10(b) there are only two and so this structure would be expected to be semiconducting. The model in Fig. 10(b), however, dictates a stronger correlation between the rows of ad-dimers. The calculations of Seino and Ishii predicted that only one maximum should appear in STM images of Ag-Ge dimers, consistent with our observations.

V. SUMMARY

Silver growth on Ge(100) was studied as a function of coverage and substrate temperature using STM. At 330 K, 2D island growth competed with 3D cluster growth. There were two types of 2D islands, one elongated perpendicular to the Ge dimer rows the other parallel; the latter predominated. The former were attributed to Ag adatoms attaching across the substrate dimer bond while the latter may be due to parallel Ag ad-dimers. The 3D clusters were (110)-oriented Ag with Ag[001] parallel to the Ge $2\times$ direction. Annealing above 470 K caused the 2D islands to disappear and the 3D cluster density to decline drastically. Depositing the Ag film at 470 K created two types of metastable Ag-Ge surface structures. These islands exhibited 3×2 and 2×3 periodicities and appeared simultaneously with pits in the Ge surface which was taken as an indication that the islands were 2D Ag-Ge surface alloys. A model for the 3×2 structure based on Ag substitution into the Ge surface and Ag-Ge ad-dimers was proposed. Both the 3×2 and 2×3 structures could only be seen following Ag growth at 470 K. Higher growth temperatures, annealing films grown at lower temperatures to 470 K, and even holding the surface at 470 K following

growth at the same temperature, all led to only 3D clusters.Thus the formation of the 3×2 and 2×3 surface alloys was attributed to growth of metastable Ag-Ge nuclei at 470 K. At lower temperatures, the Ag-Ge nuclei could not form while at higher temperatures they were too short lived to grow.

ACKNOWLEDGMENTS

The authors acknowledge the assistance of M. Li, W. Gao, R. E. Tanner, and G. Zheng in carrying out this work. This project was supported by the National Science Foundation under Grant No. CTS-9733416.

[1] F. Komori, K. Kushida, K. Hattori, S. Arai, and T. Iimori, Surf. Sci. **438**, 123 (1999).
[2] K. Kushida, K. Hattori, S. Arai, T. Iimori, and F. Komori, Surf. Sci. **442**, 300 (1999).
[3] J. R. Lince, J. G. Nelson, and R. S. Williams, J. Vac. Sci. Technol. B **1**, 553 (1983).
[4] T. Miller, E. Rosenwinkel, and T.-C. Chiang, Phys. Rev. B **30**, 570 (1984).
[5] T. Miller, E. Rosenwinkel, and T.-C. Chiang, Solid State Commun. **50**, 327 (1984).
[6] T. B. Massalski (ASM International, Materials Park, Ohio, 1990).
[7] X. F. Lin, K. J. Wan, and J. Nogami, Phys. Rev. B **49**, 7385 (1994).
[8] G. Le Lay, Surf. Sci. **132**, 169 (1983).
[9] W. C. A. N. Ceelen *et al.*, Appl. Surf. Sci. **134**, 87 (1998).
[10] L. H. Chan and E. I. Altman, Phys. Rev. B **63**, 195309 (2001).
[11] L. H. Chan and E. I. Altman, Surf. Sci. (to be published).
[12] L. H. Chan, Y. Liang, and E. I. Altman, J. Vac. Sci. Technol. A **19**, 976 (2001).
[13] C. Y. Nakakura *et al.*, Rev. Sci. Instrum. **69**, 3251 (1998).
[14] K. Seino and A. Ishii, Surf. Sci. **493**, 420 (2001).
[15] D. J. Chadi, Phys. Rev. Lett. **59**, 1691 (1987).
[16] T. Sato, T. Sueyoshi, T. Amakusa, and M. Iwatsuki, Surf. Sci. **340**, 328 (1995).
[17] B. A. G. Kersten, H. J. W. Zandvliet, D. H. A. Blank, and A. van Sifhout, Surf. Sci. **322**, 1 (1995).
[18] E. Zoethout, H. J. W. Zandvliet, W. Wulfhekel, G. Rosenfeld, and B. Poelsema, Phys. Rev. B **58**, 16 167 (1995).
[19] M. Li and E. I. Altman, Phys. Rev. B **66**, 115313 (2002).
[20] C. S. Chang, Y. M. Huang, C. C. Chen, and T. T. Tsong, Surf. Sci. **367**, L8 (1996).
[21] E. I. Altman and R. J. Colton, Surf. Sci. **304**, L400 (1994).
[22] X. F. Lin, K. J. Wan, and J. Nogami, Phys. Rev. B **47**, 10 947 (1993).
[23] H. Roder, R. Schuster, H. Brune, and K. Kern, Phys. Rev. Lett. **71**, 2086 (1993).
[24] D. D. Chambliss, R. J. Wilson, and S. Chiang, J. Vac. Sci. Technol. A **10**, 1993 (1992).
[25] D. Winau, H. Itoh, A. K. Schmid, and T. Ichinokawa, Surf. Sci. **303**, 139 (1994).
[26] T. Michely, M. C. Reuter, M. Copel, and R. M. Tromp, Phys. Rev. Lett. **73**, 2095 (1994).
[27] H. W. Yeom, I. Matsuda, K. Tono, and T. Ohta, Phys. Rev. B **57**, 3949 (1998).
[28] M. Shimomura *et al.*, Surf. Rev. Lett. **5**, 953 (1998).